DNAJA1 dysregulates metabolism promoting an anti-apoptotic phenotype in pancreatic ductal adenocarcinoma

Heidi Roth
University of Nebraska-Lincoln
Fatema Bhinderwala
University of Nebraska-Lincoln
Rodrigo Franco
University of Nebraska-Lincoln
You Zhou
University of Nebraska-Lincoln
Robert Powers (rpowers3@unl.edu)
University of Nebraska-Lincoln https://orcid.org/0000-0001-9948-6837

Research

Keywords: Pancreatic cancer, metabolomics, NMR, DNAJA1, glycolysis, co-chaperones

DOI: https://doi.org/10.21203/rs.3.rs-76631/v1

Abstract

Background

At less than 7%, pancreatic ductal adenocarcinoma (PDAC) has one of the poorest 5-year cancer survival rates and is set to be the leading cause of cancer related deaths by 2030. The co-chaperone protein DNAJA1 (HSP40) is downregulated four-fold in pancreatic cancer cells, but its impact on pancreatic ductal adenocarcinoma (PDAC) progression remains unclear.

Methods

DNAJA1 was overexpressed in pancreatic cancer cell lines, BxPC-3 and MIA PaCa-2, through retroviral transfection. The impact of overexpressing DNAJA1 was investigated using a combination of untargeted metabolomics, stable isotope resolved metabolomics (SIRM), confocal microscopy, flow-cytometry, and cell-based assays.

Results

Pancreatic cancer cells overexpressing DNAJA1 exhibited a global metabolomic change. Specifically, differential output from Warburg glycolysis, an increase in redox currency, and an alteration in amino acid levels were observed in both overexpression cell lines. DNAJA1 overexpression also led to mitochondrial fusion, an increase in the expression of Bcl-2, a modest protection from redox induced cell death, a loss of structural integrity due to the loss of actin fibers, and an increase in cell invasiveness in BxPC-3. These differences were more pronounced in BxPC-3, which contains a loss-of-function mutation in the tumor suppressing gene SMAD4.

Conclusions

The overexpression of DNAJA1 promoted cellular proliferation, redox tolerance, invasiveness, and anti-apoptosis, which suggests DNAJA1 has numerous regulatory roles. Overall, our findings suggest a proto-oncogenic role of DNAJA1 in PDAC progression and suggests DNAJA1 may function synergistically with other proteins with altered activity in pancreatic cancer cell lines.

Full Text

Due to technical limitations, full-text HTML conversion of this manuscript could not be completed. However, the manuscript can be downloaded and accessed as a PDF.

Figures

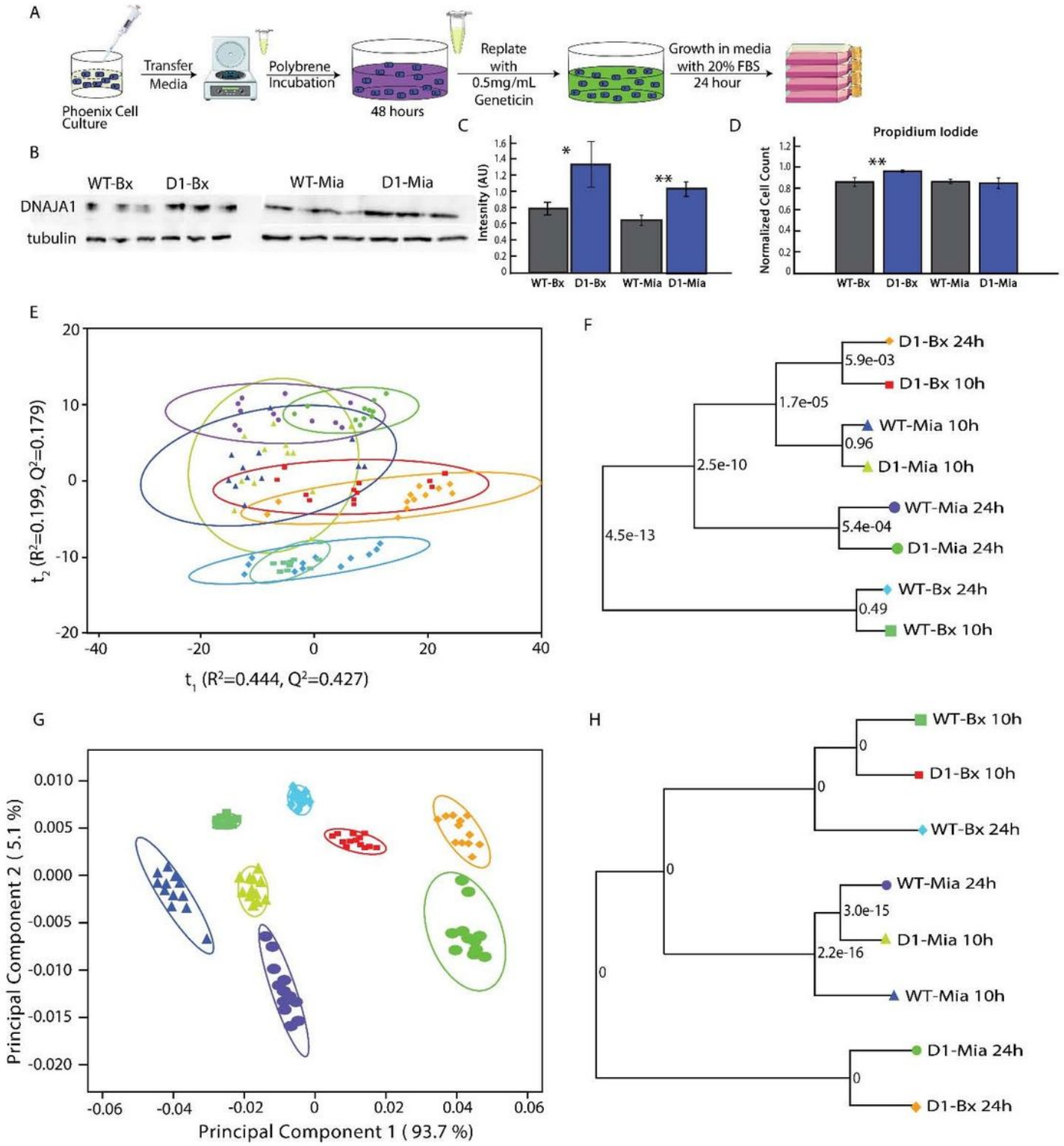

Figure 1

DNAJA1 overexpression imparts a unique metabolic profile in pancreatic cancer cells (A) Schematic summarizing the generation of stable DNAJA1 overexpressing PDAC cells. (B) Western immunoblot analysis showing the successful overexpression of DNAJA1. Images in this figure are free medical images from Servier Medical Art (https:/smart.servier.com/) under the Creative Commons License Attribution 3.0 Unported (CC BY 3.0) (C) Bar graph quantifying the DNAJA expression in WT and D1 cells

from the Western immunoblots in A. Data are plotted as an average of triplicate measurements (n=3) with standard deviations represented as brackets. WT bars are colored gray and D1 bars are colored blue. Univariate pairwise comparisons used a Student's T-test with p-values indicated as: * $p < 0.05$ and ** $p < 0.01$. (D) PCA scores plot generated from 1D 1H NMR spectra of cell lysates of WT and D1 cell lines of BxPC-3 and MIA PaCa-2 (R2 0.643, Q2 0.606). The ellipses around each cluster corresponds to the 95% confidence interval for a normal distribution of data. Each cluster contains 12 replicates, except for WT-Bx at 10-hour where n=9 and D1-Mia at 24 hours where n=11. (E) Metabolic tree diagram generated from the PCA scores plot in D. The p-value at each node is calculated from the Mahalanobis distance between each group. The coloring is identical between the PCA scores plot and the tree diagram. (F) PCA scores plot generated from peak intensities in the 2D 1H-13C NMR spectra for cell lysates of both WT and D1 cell lines (R2 0.989, Q2 0.988). (G) Metabolic tree diagram generated from the PCA scores plot in F. The color scheme is. WT-Bx cells at 10 hours () and at 24 hours (), and D1-Bx cells at 10 hours () and at 24 hours (). Similarly, WT-Mia at 10 hours () and at 24 hours (), and D1-Mia at 10 hours () and at 24 hours ().

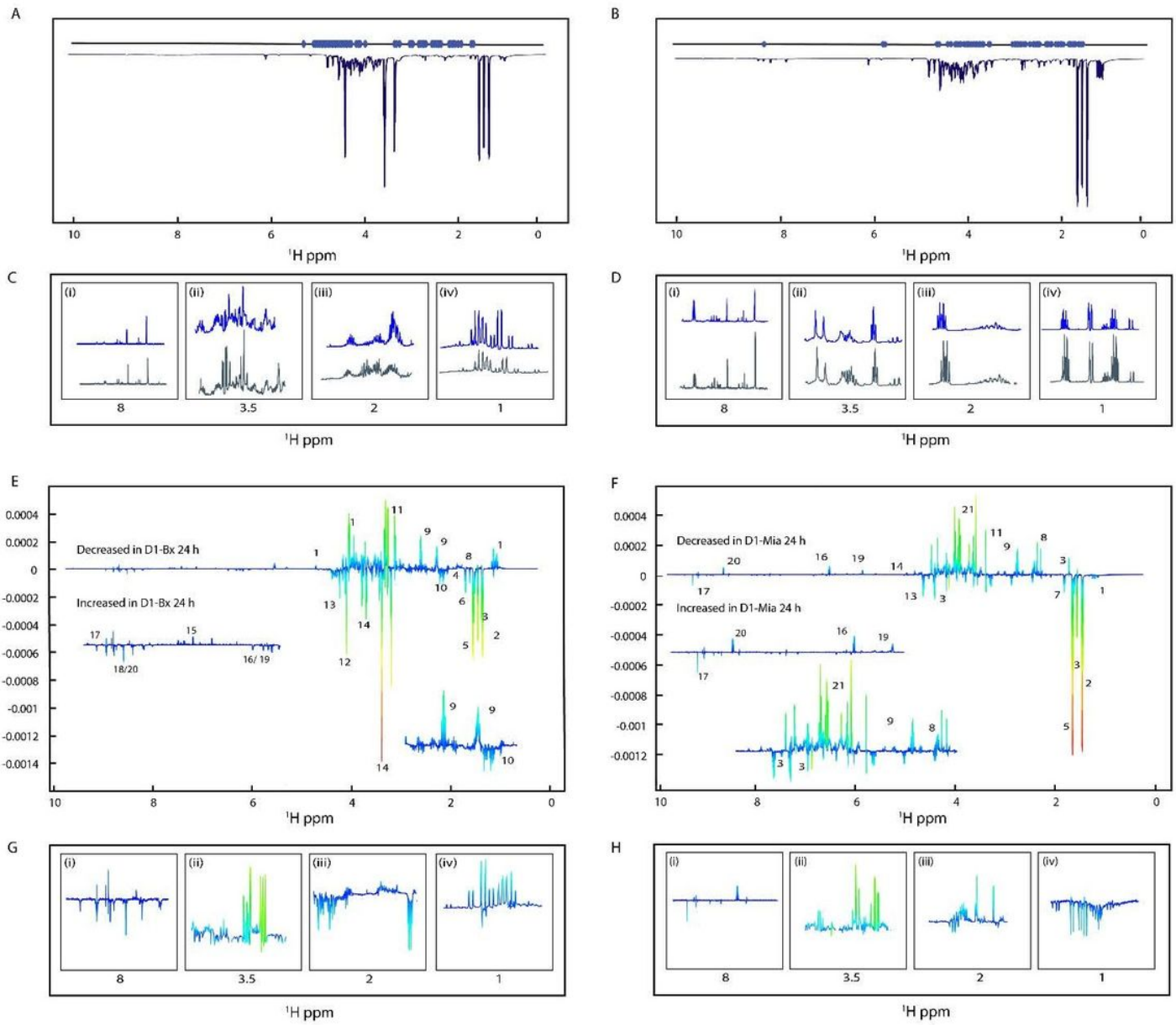

Figure 2

Global metabolic changes observed following DNAJA1 overexpression 37 Spectral variations between WT and D1 cells. A mean 1D 1H NMR spectrum of wild-type (A) BxPC-3 and (B) MIA PaCa-2 cells are marked with red points indicating the significantly altered ($p < 0.001$) NMR spectral bins in the corresponding 1D 1H NMR spectrum for D1 cells. Expanded views of mean 1D 1H NMR spectrum with WT shown in gray (bottom) and D1 shown in blue (top) for (C) WT-Bx and D1-Bx, and (D) WT-MIA and D1-Mia. The panels in C and D correspond to: (i) branched chain amino acids, (ii) glutamine and glutamate, (iii) glucose, and (iv) energy metabolites. Back-scaled loadings plot comparing (E) WT-Bx to D1-Bx, and (F) WT-Mia to D1-Mia at the 24-hour time point. The back-scaled loadings plot in E and F were generated from valid OPLS-DA models: R2 0.999, Q2 0.982, CV-ANOVA p-value 1.2x10-13 and R2 0.997, Q2 0.989, CV-ANOVA p-value 7.27x10-14, respectively. Positive peaks identify spectral features increased in WT and negative peaks are decreased in WT. Peaks observed in the back-scaled plots are numbered as follows: 1, branched chain amino acids (leucine, isoleucine, valine); 2: lactate, 3: alanine, 4: acetate, 5: 3-hydroxybutyrate 6: aminobutyrate 7: lysine 8: arginine, 9: glutamine 10: glutamate 11: aspartate 12: cystathionine, 13: proline, 14: glucose 15: aromatic amino acids (tyrosine and phenylalanine), 16: NADP+, 17: NADH, 18: AXP, and 19: CXP ,20: UXP and UXP-glucose 21: Myo-inositol. (G and H) Expanded views of the back-scaled loadings plots of E and F, respectively. The panels in G and H correspond to: (i) branched chain amino acids, (ii) glutamine and glutamate, (iii) glucose, (iv) energy metabolites.

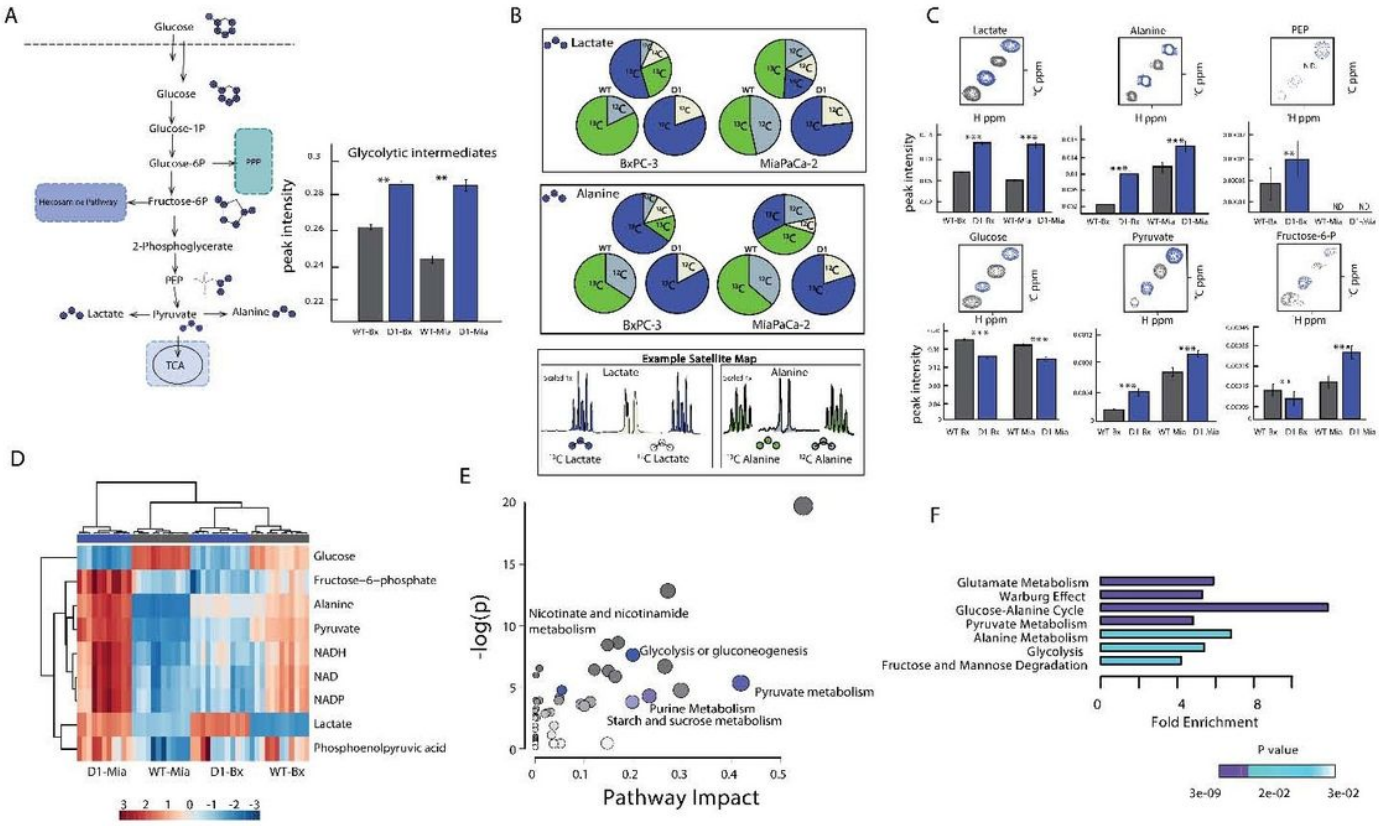

Figure 3

DNAJA1 alters aerobic glycolysis and encourages diverse glucose utilization (A) (left) A schematic of the glycolytic pathway, which illustrates the major regulatory steps, the location of 13C carbons in metabolites derived from 13C6-glucose, and the metabolic products of aerobic glycolysis. The blue circles overlaid on the chemical structures identify the location of 38 13C-carbons. (right) A bar graph plotting the sum of NMR peak intensities for all glycolytic intermediates obtained from 2D 1H-13C HSQC spectra. WT bars are colored gray and D1 bars are colored blue. A statistically significant increase in glycolysis resulted from DNAJA1 overexpression. (B) Pie charts summarizing the fractional 13C enrichment of lactate (top panel) and alanine (middle panel) catabolized from 13C6-glucose. The fractional 13C enrichment was determined from the 13C satellite peaks in 1D 1H NMR spectra. Fractions of 12C- and 13C –metabolite are represented by each arc-length. The pie charts corresponding to: WT (bottom left pie chart) are colored green for 13C and gray for 12C, D1 (bottom right chart) are colored blue for 13C and cream for 12C, and WT + D1 (top middle pie chart) is a composite of the two bottom pie charts using the same color scheme as the individual WT and D1 pie charts. (bottom panel) Expanded view of representative 1D 1H NMR spectra highlighting selected (left) lactate and (right) alanine 1H-12C and 1H-13C peaks. The 13C-satelites are scaled relative to the 1H-12C peaks. The 13C-satelites are colored blue for lactate and green for alanine. The 1H-12C peaks are colored cream for lactate and gray for alanine. The same color scheme is used to highlight the 12C and 13C atoms in the chemical structures below the NMR spectra. A variable enrichment in 13C6-glucose-derived 13C-lactate and 13C-alanine resulted from DNAJA1 overexpression. (C) Expanded view of overlaid 2D 1H-13C HSQC spectra and the associated bar charts for WT and D1 cells. Bar charts highlight the significant metabolic shift in metabolites derived from 13C glucose. Data are plotted as the average peak intensity from 2D 1H-13C HSQC spectra with standard deviations represented as brackets (n=12). WT bars and HSQC peak contours are colored gray and D1 bars and HSQC peak contours are colored blue. (D) Heat map and hierarchical clustering of glycolytic intermediates. Heat map plots normalized peak intensities from 2D 1H-13C HSQC spectra. Each row displays the relative metabolite abundance across the four groups, where red identifies a relative metabolite accumulation and blue indicates metabolite depletion. (E) Pathway impact plot based on metabolite occurrence from the analysis of the 2D 1H-13C HSQC spectra. (F) Pathway enrichment plot based on metabolite concentrations from the analysis of the 2D 1H-13C HSQC spectra. Pathway fold enrichment is colored according to the corresponding p-value using the indicated purple to teal scale. Pathways were selected to highlight the intracellular metabolic variations linked to glucose metabolism. See Supplemental Figure 4 for the complete list of pathways enriched by DNAJA1 overexpression. The pathway impact and enrichment plots were generated using MetaboAnalyst 4.0 (https://www.metaboanalyst.ca/). Univariate pairwise comparisons used a Student’s T-test followed by a Benjamini-Hochberg multiple-hypothesis correction. The corrected p-values are indicated as: * $p < 0.05$, ** $p < 0.01$, *** $p < 0.001$, and # $p < 0.0001$.

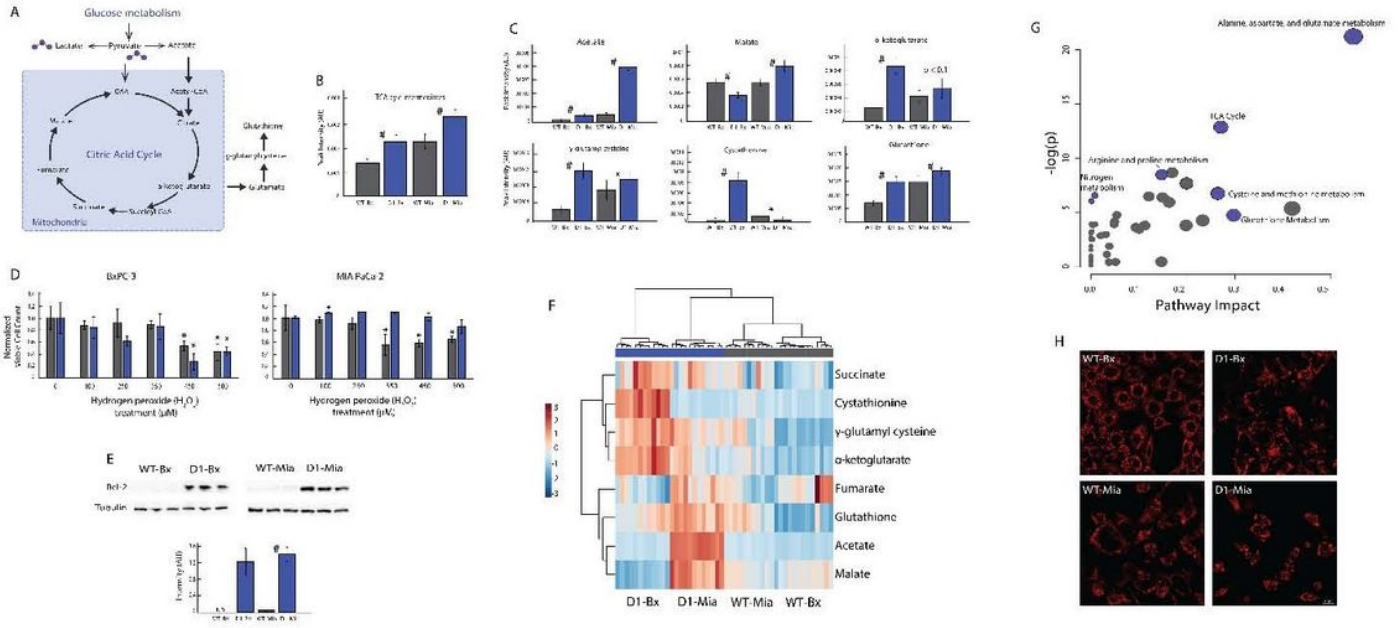

Figure 4

Disrupted redox balance fueled by an increase in TCA cycle activity in D1 overexpression (A) A schematic of the TCA cycle illustrating the incorporation of 13C-carbons from glycolysis (i.e., from 13C6-glucose) into TCA intermediates, and the flow of metabolites into and out of the mitochondria. (B) A bar graph plotting the sum of NMR peak intensities for all 3C6-glucose-derived TCA cycle intermediates obtained from 2D 1H-13C HSQC spectra. WT bars are colored gray and D1 bars are colored blue. A statistically significant increase in TCA cycle intermediates resulted from DNAJA1 overexpression. (C) Bar charts highlight the significant metabolic shift in TCA cycle metabolites derived from 13C glucose as a result of DNAJA1 overexpression. Data are plotted as the average peak intensity from 2D 1H-13C HSQC spectra with standard deviations represented as brackets (n=12). WT bars are colored gray and D1 bars are colored blue. (D) Bar graph of XTT survivability assay plotted over a range (0 to 500 M) of hydrogen peroxide treatments. Data are plotted as an average of triplicate measurements (n=3) with standard deviations represented as brackets. WT bars are colored gray and D1 bars are colored blue. (E) Western blot (top) analysis and bar graph quantification (bottom) of Bcl-2 induction due to DNAJA1 overexpression. Data are plotted as an average of triplicate measurements (n=3) with standard deviations represented as brackets. ND: no data. (F) Heat map and hierarchical clustering of TCA cycle intermediates. Heat map plots normalized peak intensities from 2D 1H-13C HSQC spectra. Each row displays the relative metabolite abundance across the four groups, where red identifies a relative metabolite accumulation and blue indicates metabolite depletion. (G) Pathway impact plot based on metabolite occurrence from the analysis of the 2D 1H-13C HSQC spectra. Pathways were selected to highlight the intracellular metabolic variations linked to glucose metabolism. See Supplemental Figure 4 for the complete list of pathways enriched by DNAJA1 overexpression. The pathway impact plot was generated using MetaboAnalyst 4.0 (https://www.metaboanalyst.ca/). (H) Live-cell confocal microscopy

images of mitochondria from WT and D1 cells using Mitotracker Red. Univariate pairwise comparisons used a Student's T-test followed by a Benjamini- Hochberg multiple-hypothesis correction. The corrected p-values are indicated as: * $p < 0.05$, ** $p < 0.01$, *** $p < 0.001$, and # $p < 0.0001$.

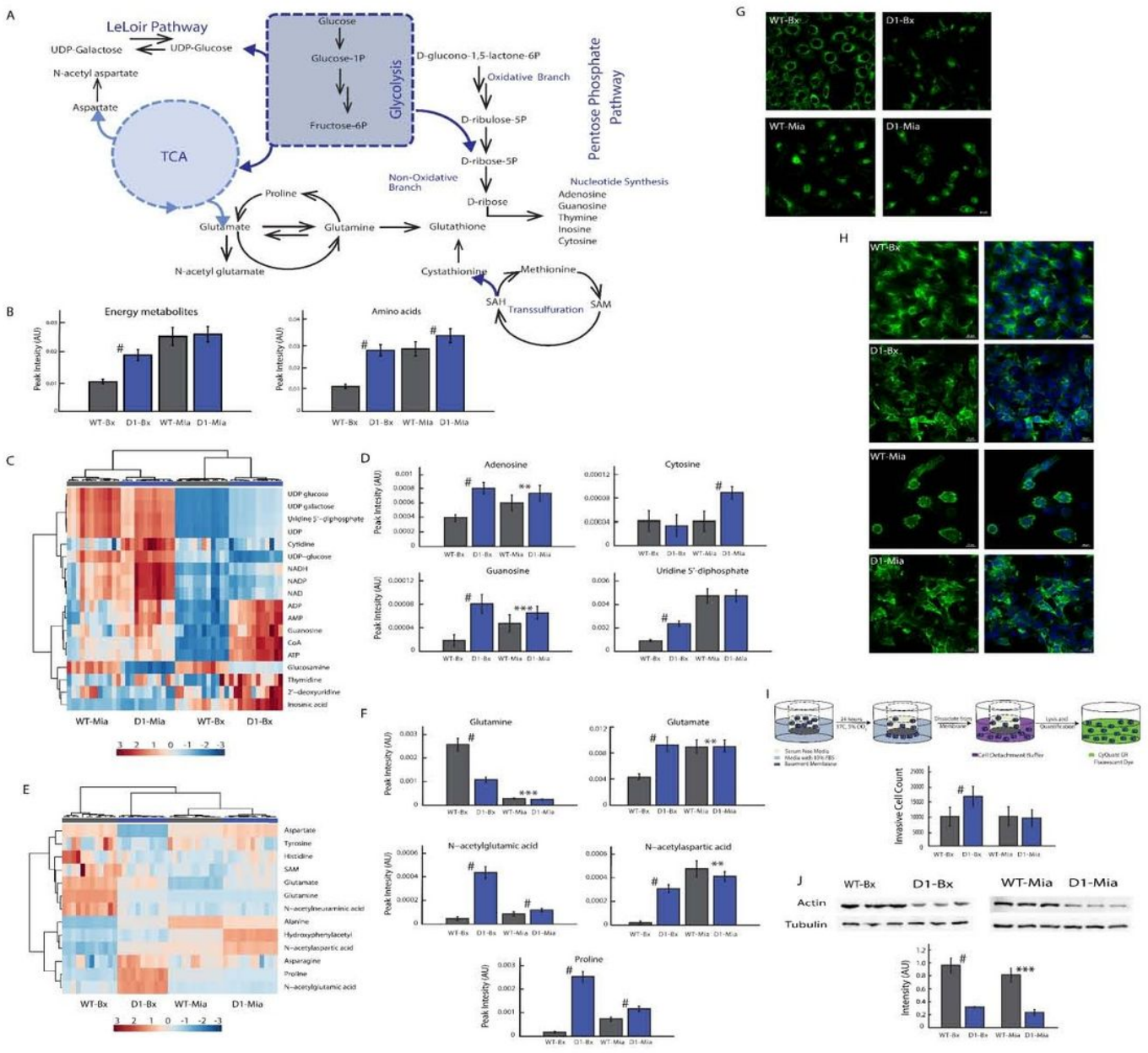

Figure 5

Aberrant amino acid metabolism coupled to a loss of cell structure results in an increase in cell invasiveness from DNAJA1 overexpression (A) Illustration of the metabolic network that encompasses the biosynthesis of nucleotides and amino acid (e.g., Glycolysis, Leloir pathway, Pentose Phosphate Pathway, TCA cycle, etc.). The metabolic network identifies possible pathways of 13C-carbon incorporation into amino acids and nucleotides as derived from 13C6-glucose. (B) Bar graphs plotting the sum of NMR peak intensities for all 13C6-glucose-derived nucleotides (i.e., energy metabolites) and

amino acid intermediates obtained from 2D 1H-13C HSQC spectra. WT bars are colored gray and D1 bars are colored blue. A statistically significant increase in nucleotides and amino acids was observed for D1-Bx, while only a modest increase in amino acids occurred for D1-Mia. Heat map and hierarchical clustering analysis of (C) nucleotides and (E) amino acid intermediates. Heat map plots normalized peak intensities from 2D 1H-13C HSQC spectra (n=12, n=11 for WT-Bx). Each row displays the relative metabolite abundance across the four groups, where red identifies a relative metabolite accumulation and blue indicates metabolite depletion. Bar charts highlight the significant metabolic shift in (D) nucleotides and (F) amino acids derived from 13C6-glucose. Data are plotted as the average peak intensity from 2D 1H-13C HSQC spectra with standard deviations represented as brackets (n=12). (G) Live-cell confocal microscopy images of lysosomes from WT and D1 cells using lysotracker deep red. (H) Fixed-cell confocal microscopy images of actin filament variations between WT and D1 cells. (I) (top) Schematic of the invasion assay methodology. (bottom) Bar graph quantitation of cell invasiveness. Data are plotted as the number of cells present in the basement membrane with standard deviations represented as brackets (n=3). (J) Western blot (top) analysis and bar graph quantification (bottom) of actin expression in WT and D1 cells. Data are plotted as an average of triplicate measurements (n=3) with standard deviations represented as brackets. Univariate pairwise comparisons used a Student's T-test followed by a Benjamini- Hochberg multiple-hypothesis correction. The corrected p-values are indicated as: * $p < 0.05$, ** $p < 0.01$, *** $p < 0.001$, and # $p < 0.0001$.

Supplementary Files

This is a list of supplementary files associated with this preprint. Click to download.

- rpowerssupplementalinformation.pdf